A prototype acoustic gas sensor based on attenuation (L)

Andi Petculescu[a)]
Department of Mechanical Engineering, Northwestern University, 2145 Sheridan Road, Evanston, Illinois 60208

Brian Hall, Robert Fraenzle, and Scott Phillips
Commercial Electronics, Broken Arrow, Oklahoma 74012

Richard M. Lueptow
Department of Mechanical Engineering, Northwestern University, 2145 Sheridan Road, Evanston, Illinois 60208

(Received 27 March 2006; revised 21 July 2006; accepted 21 July 2006)

Acoustic attenuation provides the potential to identify and quantify gases in a mixture. We present results for a prototype attenuation gas sensor for binary gas mixtures. Tests are performed in a pressurized test cell between 0.2 and 32 atm to accommodate the main molecular relaxation processes. Attenuation measurements using the 215-kHz sensor and a multiseparation, multifrequency research system both generally match theoretical predictions for mixtures of CO_2 and CH_4 with 2% air. As the pressure in the test cell increases, the standard deviation of sensor measurements typically decreases as a result of the larger gas acoustic impedance. © *2006 Acoustical Society of America.* [DOI: 10.1121/1.2336758]

PACS number(s): 43.35.Fj, 43.35.Yb [RR] Pages: 1779–1782

I. INTRODUCTION

The propagation of acoustic waves in gases is intimately linked to gas composition, temperature, and pressure. This may enable the use of acoustic waves as a quantitative probe of the thermodynamic and molecular properties of gas mixtures. The classical sound attenuation arises by transport phenomena (e.g., heat conduction, viscosity, and diffusion) while the nonclassical absorption is due to thermal relaxation involving the molecules' vibrational and rotational levels. In a gaseous medium, the molecules exchange energy via collisions. In the absence of any external perturbations, the internal degrees of freedom of the gas molecules (e.g., vibration and rotation) are rapidly thermalized. As a result, the gas is in thermal equilibrium at a constant temperature. When an acoustic wave is launched in the gas, this equilibrium is broken: the internal degrees of freedom (DOF) activated by collisions now have to relax to the acoustic temperature. Generally speaking, the wave energy expended to activate the molecular internal degrees of freedom is not promptly returned to the acoustic wave. This gives rise to a net absorption of acoustic energy—the nonclassical, or molecular absorption of sound. The sound absorption is largest when the acoustic period is commensurate with the molecular relaxation time. It is this feature that makes acoustic studies of molecular relaxation possible.

Over the years, many carefully thought-out experiments have been designed for the accurate measurement of attenuation and sound speed, only a few of which are mentioned here.[1–10] In his book, Lambert[11] describes various acoustic experimental techniques to measure molecular relaxation. The experiments, coupled with a strong modeling effort, have yielded insights into the physical mechanisms responsible for molecular relaxation in various gas mixtures.

Typical acoustic gas monitors operate by tracking changes in the adiabatic sound speed c that are induced largely by changes in the molecular weight according to the ideal-gas formula $c=\sqrt{\gamma RT/M}$, where $\gamma=C_P/C_V$ is the isobaric-to-isochoric specific heat ratio, $R=8.3144$ J/mol/K is the universal gas constant, T is the ambient temperature, and M is the molecular weight of the gas. For some applications requiring a quantitative analysis of the monitored environment, the speed of sound alone cannot provide sufficient information. That is where measurements of the acoustic attenuation come into play. As shown in our previous work,[12] precise measurements of sound speed *and* attenuation can lead to (quasi) quantitative gas analysis via the identification of the molecular symmetry properties, if not of the molecules themselves. In the future, this could lead to the development of rugged "smart" acoustic sensors capable of quantitatively determining gas composition in various environments and processes.

In this paper we report on the development of a prototype dual-path acoustic sensor assembly that measures the acoustic attenuation in gas mixtures. From an experimental standpoint, the main challenge is extracting the acoustic attenuation from only two fixed-length sensing paths, as opposed to multiple-separation measurements where the separation distance between the emitting and receiving transducers is increased incrementally.[9] To compare the two cases, measurements are performed inside a pressurized test cell for different gas mixtures. Since relaxation times vary inversely with ambient pressure,[13] decreasing the pressure p is equivalent to increasing the frequency f and vice versa. By changing the pressure in the test cell incrementally over al-

[a)]Currently at University of Louisiana at Lafayette, Department of Physics; electronic mail: andi@louisiana.edu

most two orders of magnitude, we attained an f/p range that is wide enough to cover the main molecular relaxation processes of the gas mixtures.

II. THEORETICAL MODEL

In the theoretical model,[14–16] we fit a shifted-exponential function to the Lennard-Jones interaction potential[17] to obtain the transition probabilities between vibrational levels. For gas mixtures containing at least one polyatomic (thus relaxing) component, this is done for *each* energy exchange process,[14] whether interspecies or intraspecies. The fact that there exists a time delay or phase shift between the acoustic fluctuations and the exchange of energy from the internal to the external DOF makes the specific heat per mole complex-valued and frequency- dependent, i.e., it becomes an *effective specific heat*, $C_V^{\text{eff}}(f)$. The subscript V denotes isochoric processes. Using the equations of linear acoustics coupled with the equations for molecular relaxation, we have shown that the propagation of sound in excitable gas mixtures is ultimately characterized by the *effective wave number*,[14] $\tilde{k}(f)=2\pi f\sqrt{\rho_0 p_0^{-1} C_V^{\text{eff}}(f)[C_V^{\text{eff}}(f)+R]^{-1}}$, where ρ_0 and p_0 are the equilibrium density and pressure of the gas. The real and imaginary parts of the effective wave number $\tilde{k}$ determine the phase velocity c and attenuation $\alpha=\alpha_{\text{class}}+\alpha_m$ of the acoustic wave,via

$$\tilde{k}(f)=\frac{2\pi f}{c(f)}-i\alpha(f),$$

where the classical attenuation, α_{class}, results from viscous, thermal, and diffusional losses, and the molecular attenuation, α_m, results from relaxation processes. A good way to emphasize relaxational effects on the acoustic attenuation is by representing the *normalized attenuation* $\alpha\lambda$, where λ is the acoustic wavelength, against the frequency-to-pressure ratio. The presence of relaxing gases is manifested by relaxational peaks in the normalized attenuation.

It is important to note that for certain gas mixtures and for certain ambient conditions of temperature and pressure, additional mechanisms such as chemical reactions[18] and thermal radiation[19] may become important and thus may need to be accounted for in the modeling. We estimated theoretically that the effect of infrared radiation on the relaxation times and sound absorption is too small to be of any importance for the gas compositions and ambient conditions encountered in these experiments. Also, if present in the sensing volume, water vapor could influence the molecular sound absorption noticeably.[20,21] Nevertheless, dry gases were used in the experiments presented here to avoid having any water vapor present.

III. APPARATUS

In order to (i) check the validity of the model and (ii) establish experimental attenuation "references" for various gas mixtures, we use a pressurized test cell connected to a precision gas mixing system. For reference measurements in the test cell, four transmitter-receiver (T/R) pairs of narrowband piezoelectric transducers operating at 92, 149, 215, and 1000 kHz are used. The transducers are mounted inside the pressure chamber on a linear translation stage enabling 75 different T/R separations measured precisely to within 0.03 mm. For each pair, one transducer is fixed while the other is incrementally displaced, thus changing the transmitter-receiver separation length. The operating frequencies are chosen such that, together with the attainable pressure range (roughly 0.2–32 atm), they provide a frequency-to-pressure ratio span that covers the primary relaxation processes for the gases of interest (methane, carbon dioxide, ethylene, nitrogen, air). A detailed description of the apparatus is given in Ref. 9.

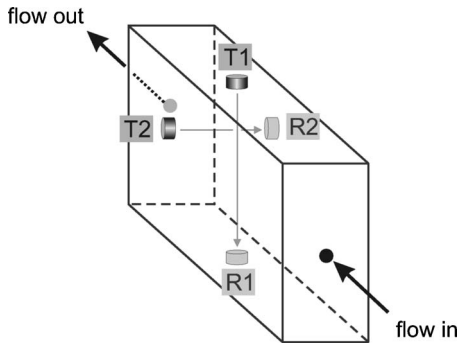

FIG. 1. Schematic diagram of the sensing geometry. The two sensing paths (T1/R1 and T2/R2) lie in planes 2 cm apart. Flow is perpendicular to both sensing paths.

The sensor assembly operates at a fixed frequency of 215 kHz. A diagram of the sensing geometry of the prototype acoustic sensor is shown in Fig. 1. The hardware consists of four ultrasonic piezoelectric transducers arranged on two sensing paths inside a small rectangular chamber (approximately 70 mm × 43 mm × 69 mm) that allows the monitored gas to flow through the sensing area. The two sensing paths, T1/R1 and T2/R2 with separation lengths of 30 and 60 mm, respectively, are staggered by 2 cm in the flow direction. Two identical end plates provide the gas inlet and outlet ports. A metal screen between the inlet and the sensing area diffuses the flow. The transmitters (T1, T2) are energized with square-wave pulse-trains of either five or ten cycles. The ultrasonic bursts travel through the gas medium to the receiving transducers (R1, R2) where they are converted to electrical signals sent to the processing electronics.

IV. DATA ANALYSIS AND RESULTS

In order to remove any dc offsets and spurious high-frequency components, a bandpass filter is applied to the signals received on the two paths. To correct for diffraction effects due to the finite size of the transmitter, the amplitude A_{rec} of each received signal is multiplied by a correction factor based on the far-field diffraction from a circular source:[9,22]

$$A(x)=A_{\text{rec}}(x)\left\{\sin\left[\frac{\pi f}{c}(\sqrt{x^2+R_E^2}-x)\right]\right\}^{-1}, \quad (1)$$

where x is the propagation distance and R_E is the emitter radius.

For the multiple-separation measurements in the test cell, 75 transmitter-receiver separations can be achieved us-

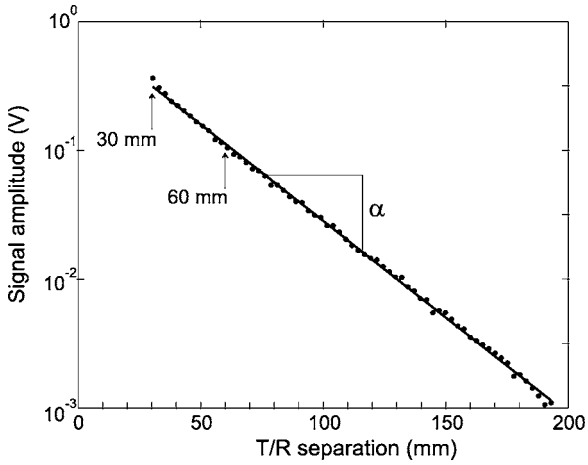

FIG. 2. Amplitude of the received signal as a function of transmitter-receiver (T/R) separation for a typical multiple-separation experiment inside the test cell. The curve is a linear fit to the 75 amplitude values. The arrows indicate the two sensing paths implemented in the sensor assembly.

ing a linear translation stage. However, the sensor prototype relies on only two sensing paths, which makes the measurements more challenging. Figure 2 shows the signal amplitude (in volts) as a function of transmitter-receiver separation for a typical multiple-separation experiment, along with the values for the two sensing paths implemented in the sensor (arrows). A linear fit is sought for the logarithmic amplitude versus separation length, whose slope yields the attenuation coefficient α.[9] In the test cell, the linear fit is based on many data points (typically 75 T/R separations), whereas the fit is based on only two data points for the prototype sensor. It is useful to note that the sound speed c enters the normalized attenuation (i) via the diffraction correction (1) and (ii) via the wavelength $\lambda = cf^{-1}$. In the analysis of the sensor data, we use the theoretical frequency-dependent phase velocity obtained using the above-described model.

Figures 3 and 4 show multiple-separation, multifrequency measurements of the normalized attenuation in the test cell, along with model predictions for N_2-C_2H_4 mixtures and for air-CH_4 and air-CO_2 mixtures, respectively. There is a good agreement between the experimental data and the

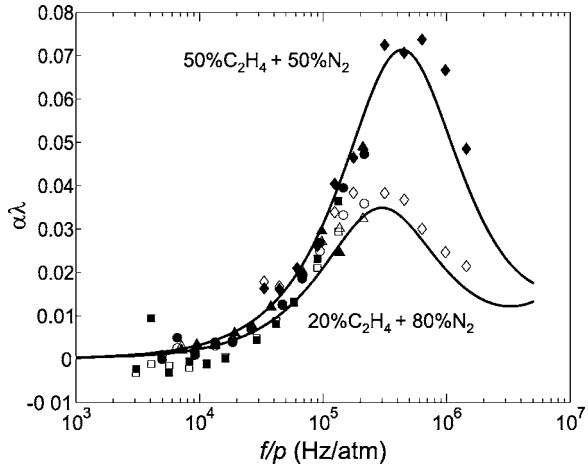

FIG. 3. Multiple-separation, multifrequency, test-cell measurements of the normalized attenuation for mixtures of 50% and 20% ethylene in nitrogen (symbols: □, 92 kHz; ○, 149 kHz; △, 215 kHz; ◇, 1 MHz; filled for 50% ethylene). Curves represent the model predictions.

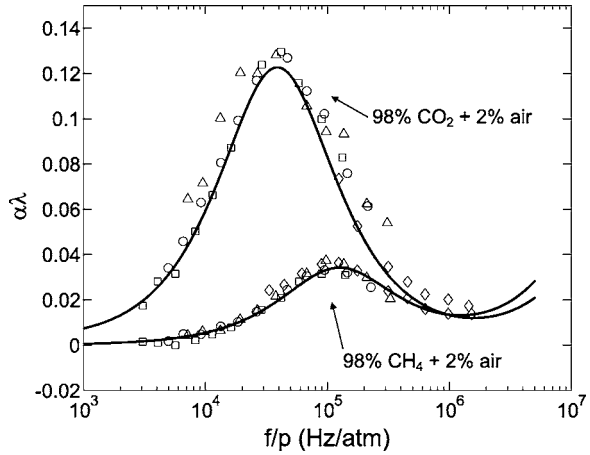

FIG. 4. Multiple-separation, four-frequency, test-cell measurements of the normalized attenuation for mixtures of CO_2 and CH_4 with air (symbols: □, 92 kHz; ○, 149 kHz; △, 215 kHz; ◇, 1 MHz). Curves represent the model predictions.

theory, especially in the region of vibrational relaxation as indicated by the normalized attenuation peaks. The vibrational modes considered in the model at room temperature are, in units of cm^{-1}:[23]

C_2H_4:	826 (rock), 943 (wag), 949 (wag), 1023 (twist), 1236 (rock), 1342 (scissor), 1444 (scissor),
CO_2:	667 (bend), 1337 (s-stretch), 2349 (a-stretch),
CH_4:	1307, 1535,
N_2:	2331.

In Fig. 3, as the ethylene concentration changes from 20% to 50%, the effective relaxation frequency shifts from 240 to 350 kHz/atm, corresponding to a decrease in the effective relaxation time from 0.66 to 0.45 μs at 1 atm, since $\tau = (2\pi f)^{-1}$.[13] This is attributed to the higher relaxational component of the 50–50 mixture, due largely to the ethylene molecules. The key point here is that the theoretical model predicts fairly well the measured attenuation, an important result given the large number of significant vibrational modes of ethylene. Prior to this, the model was only applied to gases with one to three significant vibrational modes.[9] The molecular absorption of sound by the air-CO_2 mixture in Fig. 4 is visibly larger than that of the air-CH_4 mixture, owing largely to the low-lying bending mode vibrational level of CO_2.

Comparisons of the sensor dual-path data against the multiple-separation measurements are obtained by placing the sensor assembly inside the test cell and varying the pressure over the same range as in the multiple-separation measurements (0.2–32 atm). This allows precise control of the gas composition and permits testing the sensor over a wide range of f/p (including the main relaxation processes) even though the sensor operates at a single frequency. As shown in Fig. 5, the sensor is able to capture the major relaxational features for both gas mixtures. The sensor measurements match the theory quite well for the CH_4-air mixture demonstrating the ability of the dual-path arrangement to measure the attenuation nearly as well as the multiple-separation

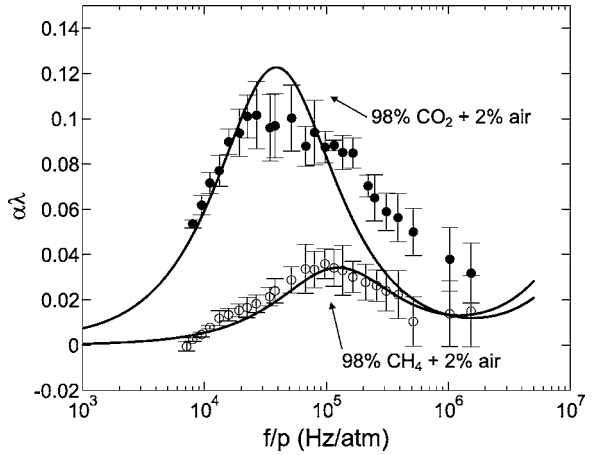

FIG. 5. Measurements with the dual-path sensor assembly at 215 kHz taken inside the test-cell over a pressure range of 0.2–32 atm (error bars represent the standard deviation over four to five tests). Curves represent the model predictions.

"laboratory" setup. The CO_2-air data are consistent with the model only in the high-pressure (small f/p) range. The departure from model predictions for the CO_2-air data at high values of f/p may stem from a number of causes. First, low-pressure measurements are challenging especially if CO_2 is present due to the high attenuation coefficient of CO_2 coupled with the large gas-transducer acoustic impedance mismatch, affecting both acoustic generation and detection. Second, any foreign molecules present in the test-cell (e.g., from small oil leaks from the vacuum pump) may induce multiple molecular relaxation pathways leading to possible broadening of the $\alpha\lambda$ curve. These issues are probably also responsible for the generally larger standard deviations at low pressures. Ambient temperature fluctuations can also affect measurements primarily via their effect on the sound speed in the medium. However, the ambient temperature varied by less than 1% during the tests so the errors introduced by temperature resulted in errors smaller than symbol sizes in Fig. 5.

V. CONCLUSIONS

We show here the basic concept for a simple dual-path acoustic gas sensor for measuring acoustic attenuation in gas mixtures. For a clear picture, we compare attenuation measurements between the dual-path, single-frequency sensor and a multiseparation, multifrequency research system for the same gas mixtures. The sensor works well, but there are limitations inherent to using only two sensing paths to obtain the attenuation coefficient, especially in the presence of a lossy gas-like CO_2. To obtain reliable quantitative real-time sensing devices, efforts must be made in the future on several fronts. In the processing electronics, filtering must be implemented in the electronics module instead of the post-processing filtering use in this analysis. Additionally, sound speed must also be measured accurately for quantitative acoustic gas sensing. For accurate time-of-flight measurements, tight thermal stability must be enforced in the sensing volume.[12] Future "smart" sensors will need to be "taught" how to interpret the acquired data based on preprogrammed physics concepts. Using sound speed and attenuation data streams, the sensor could ultimately be able to make inferences about the nature of the sensed gases based on a refined theoretical model. This constitutes a complex task, given that this is an inverse problem: it is much easier to determine sound speed and attenuation from the gas composition than vice versa. Nevertheless, combining sound speed and attenuation measurement in a simple sensor offers the potential to identify and quantify the gases making up a multicomponent mixture.

ACKNOWLEDGMENT

This work was funded by a grant from the National Aeronautics and Space Administration.

[1]F. D. Shields, "Thermal relaxation in carbon dioxide as a function of temperature," J. Acoust. Soc. Am. **29**, 450–454 (1957).
[2]T. G. Winter and G. L. Hill, "High-temperature ultrasonic measurements of rotational relaxation in hydrogen, deuterium, nitrogen, and oxygen," J. Acoust. Soc. Am. **42**, 848–858 (1967).
[3]J. C. F. Wang and G. S. Springer, "Vibrational relaxation times in some hydrocarbons in the range 300–900 K," J. Chem. Phys. **59**, 6556–6562 (1973).
[4]D. Chang, F. D. Shields, and H. E. Bass, "Sound-tube measurements of the relaxation frequency of moist nitrogen," J. Acoust. Soc. Am. **62**, 577–581 (1977).
[5]A. J. Zuckerwar and W. A. Griffin, "Resonant tube for measurement of sound absorption in gases at low frequency/pressure ratios," J. Acoust. Soc. Am. **68**, 218–226 (1980).
[6]A. J. Zuckerwar and R. W. Meredith, "Acoustical measurements of vibrational relaxation in moist N_2 at elevated temperatures," J. Acoust. Soc. Am. **71**, 67–73 (1982).
[7]J. E. Carlson and P.-E. Martinsson, "Exploring interaction effects in two-component gas mixtures using orthogonal signal correction of ultrasound pulses," J. Acoust. Soc. Am. **117**, 1961–1968 (2005).
[8]P.-E. Martinsson, "Ultrasonic measurements of molecular relaxation in ethane and carbon monoxide," Proc.-IEEE Ultrason. Symp., **511–516** (2002).
[9]S. G. Ejakov *et al.*, "Acoustic attenuation in gas mixtures with nitrogen: Experimental data and calculations," J. Acoust. Soc. Am. **113**, 1871–1879 (2003).
[10]A. Cottet *et al.*, "Acoustic absorption measurements for characterization of gas mixing," J. Acoust. Soc. Am. **116**, 2081–2088 (2004).
[11]J. D. Lambert, *Vibrational and Rotational Relaxation in Gases* (Clarendon, Oxford, 1977).
[12]A. Petculescu and R. M. Lueptow, "Synthesizing primary molecular relaxation processes in excitable gases using a two-frequency reconstructive algorithm," Phys. Rev. Lett. **94**, 238301 (2005).
[13]K. F. Herzfeld and T. H. Litovitz, *Absorption and Dispersion of Ultrasonic Waves* (Academic Press, 1959), Sec. 37.
[14]A. Petculescu and R. M. Lueptow, "Fine-tuning molecular acoustic models: Sensitivity of the predicted attenuation to the Lennard-Jones parameters," J. Acoust. Soc. Am. **117**, 175-184 (2005).
[15]Y. Dain and R. M. Lueptow, "Acoustic attenuation in three-component gas mixtures—Theory," J. Acoust. Soc. Am. **109**, 1955–1964 (2001).
[16]Y. Dain and R. M. Lueptow, "Acoustic attenuation in a three-gas mixture—Results," J. Acoust. Soc. Am. **110**, 2974–2979 (2001).
[17]R. N. Schwartz, Z. I. Slawsky, and K. F. Herzfeld, "Calculation of vibrational relaxation times in gases," J. Chem. Phys. **20**, 1591–1599 (1952).
[18]Reference 13, pp. 138–156.
[19]T. H. Ruppel and F. D. Shields, "Sound propagation in vibrationally excited N_2/CO and H_2/He/CO gas mixtures," J. Acoust. Soc. Am. **87**, 1134–1137 (1990).
[20]A. J. Zuckerwar and W. A. Griffin, "Effect of water vapor on sound absorption in nitrogen at low frequency/pressure ratios," J. Acoust. Soc. Am. **69**, 150–154 (1981).
[21]A. J. Zuckerwar and K. W. Miller, "Vibrational-vibrational coupling in air at low humidities," J. Acoust. Soc. Am. **84**, 970–977 (1988).
[22]J. M. M. Pinkerton, "On the pulse method of measuring ultrasonic absorption in liquids," Proc. Phys. Soc. London **62**, 286–299 (1949).
[23]NIST Chemistry WebBook (http://webbook.nist.gov/chemistry), accessed 20 December 2005.